

Intramolecular H-Bonds: DFT and QTAIM Studies on 3-(Aminomethylene)pyran-2,4-dione and Its Derivatives

Slawomir Janusz Grabowski* and Magdalena Małecka

Department of Crystallography and Crystal Chemistry, University of Łódź,
Pomorska 149/153, 90 236 Łódź, Poland

Received: August 3, 2006; In Final Form: September 3, 2006

Intramolecular N–H···O hydrogen bonds in 3-(aminomethylene)pyran-2,4-dione and its simple derivatives (F, Li, and BeH substituents) were analyzed theoretically. The systems were optimized at the B3LYP/6-311++G(d,p) level of approximation. For some fluorine derivatives the corresponding tautomers with O–H···N intramolecular H-bonds were investigated, and for such pairs of tautomers, the calculations on transition states of the N–H···O ⇌ N···H–O proton-transfer reaction were carried out. The geometrical and energetic parameters for these species were characterized. The topological parameters derived from Bader theory were also analyzed; these are characteristics of H-bond critical points and also of ring critical points. Besides N–H···O and O–H···N intramolecular hydrogen bonds, there are the other intramolecular interactions, mostly ionic such as Be^{+δ}···^{−δ}O, Li^{+δ}···^{−δ}O, and Li^{+δ}···^{−δ}F. The F···O interactions also exist for some of species investigated. They may be classified as energetically stabilizing ones since the corresponding bond paths and critical points exist. The numerous correlations and dependencies between geometrical, topological, and energetic parameters were detected and described.

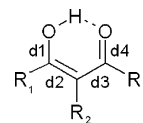
Introduction

Intramolecular hydrogen bonds are usually reported as very important interactions which often exist in all states of matter and which influence on species' properties.^{1–3} It was even claimed that in crystal structures there are preferences to form six-membered pseudo-rings closed through intramolecular H-bonds. These interactions are preferred over the other even strong intermolecular hydrogen bonds.⁴ Particularly homonuclear intramolecular O–H···O hydrogen bonds with the system of conjugated single-double bonds are often investigated (Scheme 1). For such species there is the π -electron delocalization and the enhancement of H-bond strength.⁵ Early on such interactions were classified as resonance assisted hydrogen bonds (RAHBs), and their characteristics were analyzed in detail.⁶

O–H···O RAHBs strengthened by π -electron delocalization as well as by the pseudo-ring existence possess different detectable properties. These are as follows: equalization of C–C and C=C bonds on one hand and such equalization of C–O and C=O bonds on the other hand, movement of the proton to the middle of O···O distance in extreme cases of very strong hydrogen bonds, etc. Also heteronuclear N–H···O intramolecular RAHBs were analyzed,^{7,8} as well as intermolecular RAHBs.⁹ In the latter case both homonuclear O–H···O as well as heteronuclear H-bonds, as for example N–H···O ones, are known. Numerous studies were performed on such interactions existing in carboxylic acids and amides.⁹

It is worth mentioning that the idea of resonance-assisted H-bonds was criticized recently.¹⁰ It was pointed out that neither the coupling constants nor the proton chemical shifts for species with intramolecular O–H···O and N–H···N hydrogen bonds in malonaldehyde and its diaza derivative, respectively, prove the systems' stabilization assisted by resonance. The authors claim that there are stronger H-bonds for these systems than

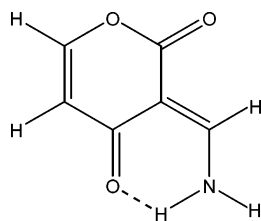
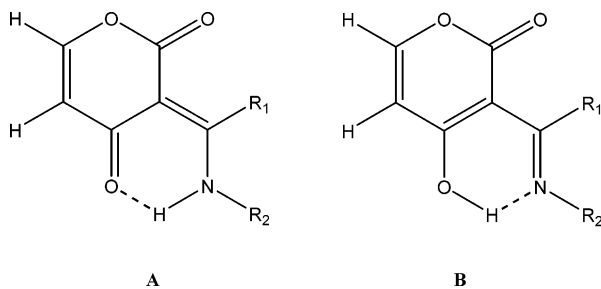
SCHEME 1



for their saturated analogues, but it is connected with the σ -skeletons of the unsaturated molecules which allow the donor and the acceptor atoms to be closer than in the corresponding saturated systems. This is in line with other studies since the MP2/6-311++G(d,p) calculations were performed on the intramolecular H-bonds for malonaldehyde and its simple chloro and fluoro derivatives,⁵ and it was found that the main part of the H-bond energy is connected with the closure of six pseudo-ring and only part of the 20–30% with the π -electron delocalization. However one can see that the latter effect is not meaningless for so-called RAHBs and undoubtedly it contributes to the enhancement of H-bond strength.

There are numerous studies on the other six-member rings. For example, these are Schiff or Mannich bases and related systems.^{2,11} Crystal structures of coumarin derivatives are the other examples.⁸ The latter compounds were also investigated theoretically since ab initio and QTAIM (quantum theory of "atoms in molecules" method)¹² calculations were performed on related systems.^{8a}

Coumarin derivatives are not convenient objects to perform the high-level calculations since they are complex species. There are two six-membered rings for them, and if additional substituents exist, the intramolecular H-bond with pseudo-ring may be also created. Thus, simpler, related species are analyzed here to deepen the nature of intramolecular interactions. There is the six-membered ring with heteroatom (oxygen) and with the oxygen attached to this ring (Scheme 2) in the species chosen for these investigations—similarly to that in coumarin. The 3-(aminomethylene)pyran-2,4-dione (Scheme 2) and its simple

SCHEME 2: 3-(Aminomethylene)pyran-2,4-dione**SCHEME 3**

derivatives are analyzed here. For such species not only intramolecular H-bonds exist but also the other intramolecular interactions.

The goal of this study is to apply density functional theory (DFT) calculations¹³ and QTAIM theory¹² to analyze the systems described. The properties of N–H···O and O–H···N H-bonds are analyzed. Also the other intramolecular interactions are investigated, and the characteristics of pseudo-rings created due to the intramolecular H-bond formation are given.

Computational Details

The calculations were performed with Gaussian03¹⁴ sets of code using the standard 6-311++G(d,p) basis set¹⁵ at the hybrid Hartree–Fock density functional (B3LYP).¹⁶ These calculations were carried out on 3-(aminomethylene)pyran-2,4-dione and its simple derivatives (Scheme 2). The following R₁ and R₂ substituents were taken into account: –H, –F, –Li, and –BeH. In the case of derivatives with R₁, R₂ = H, H; R₁, R₂ = H, F; R₁, R₂ = F, H, the tautomers where O–H···N H-bonds exist were also calculated (Scheme 3). For such pairs of tautomers the calculations were performed on transition states (TSs) of the N–H···O ⇌ N···H–O proton-transfer process. The tautomers with N–H···O hydrogen bonds are further designated as A, while their counterparts with O–H···N H-bonds as B. The results on all A and B tautomers correspond to minima since imaginary frequencies were not observed, while for TSs one imaginary frequency was detected.

QTAIM¹² is also applied here, and the characteristics of the bond critical points (BCPs) and ring critical points (RCPs) are analyzed in terms of the following properties: the electron density at the critical point (ρ_C), its Laplacian ($\nabla^2\rho_C$), and the total electron energy density at the critical point (H_C). For the latter its components are also investigated: the potential electron energy density (V_C) and the kinetic electron energy density (G_C). The following relations are well-known if all terms are expressed in atomic units.

$$1/4(\nabla^2\rho_C) = 2G_C + V_C \quad H_C = G_C + V_C \quad (1)$$

For the properties of the bond critical point and of the ring critical point the BCP and RCP subscripts are further applied here.

Results and Discussion

Relationships between Geometrical and Topological Parameters. The calculations performed on the wide spectrum of related species allow one to get deeper insight into the characteristics of intramolecular interactions. There are N–H···O and O–H···N hydrogen bonds within the species analyzed, and such interactions exist also for transition states. Hence it is possible to analyze the H···O and H···N noncovalent interactions, the covalent N–H and O–H proton donating bonds and also the “intermediate” interactions in transition states.

Tables 1 and 2 show the geometrical and topological parameters of these interactions. For example, Table 1 shows N–H bond lengths which are detected in the range of 1.019–1.044 Å, the H···N contacts are of about 1.6–1.7 Å, and H···N distances corresponding to the transition states are approximately in the range of 1.1–1.3 Å. In the case of N–H bond the electron density at the corresponding BCP amounts to ~0.3 au, for H···N interactions of TSs such electron density amounts to 0.15–0.21 au, while for H···N contacts of B tautomers the range for this quantity is 0.04–0.07 au. Besides, for two kinds of interactions, N–H bonds and H···N contacts of TSs, the corresponding Laplacian values are negative. The negative Laplacian is the topological evidence of the covalency of such interactions.^{12c,17} For H···N contacts of B tautomers Laplacians are positive as it is for the non-covalent closed shell interactions. However, even for the latter interactions, H_{BCP} values are negative which is often attributed at least to the partial covalency.¹⁷ It means that O–H···N hydrogen bonds, existing for B tautomers, are medium in strength or even they are relatively strong. It is in line with the classification of hydrogen bonds given by Rozas et al.¹⁸ The authors proposed both $\nabla^2\rho_{BCP} > 0$ and $H_{BCP} > 0$ for weak H-bonds; for medium and strong H-bonds $\nabla^2\rho_{BCP} > 0$ and $H_{BCP} < 0$, while for very strong ones both $\nabla^2\rho_{BCP} < 0$ and $H_{BCP} < 0$. This is nicely related to the Hammond–Leffler postulate.¹⁹ O–H···N H-bonds are strong since the related B tautomeric forms are close to the transition states, closer than the corresponding A tautomers where N–H···O H-bonds exist. This will be further discussed.

Similar results concerning H···O interactions are collected in Table 2. For H···O contacts corresponding to the N–H···O H-bridges in A tautomers, there are 1.7–2.3 Å distances with the electron densities at corresponding BCPs (ρ_{BCP}) of 0.01–0.04 au; Laplacians ($\nabla^2\rho_{BCP}$) are positive here, but sometimes the corresponding H_{BCP} values are negative. The latter indicates stronger interactions, partly covalent, and really H_{BCP} 's are negative for the shortest H···O contacts (for H···O = 1.710 and 1.712 Å). For the covalent O–H bonds, there are high values of electron densities at corresponding BCPs and there are negative Laplacians. For H···O interactions of transition states, the distances are equal to 1.17, 1.22, and 1.35 Å. Only for the latter case of the greatest H···O distance the Laplacian is positive but H_{BCP} is negative.

Some relationships may be observed for these parameters. Figure 1 shows the dependence between H···N/N–H and O–H/H···O distances. This is a very well-known relationship between the proton-donating bond length and the proton-acceptor distance often found for different samples of experimental and theoretical results.²⁰ It indicates that for N–H···O interactions the greater the elongation of the N–H bond is the shorter the H···O contact is; it means the stronger is the interaction. The same holds for O–H···N hydrogen bonds; the stronger interaction corresponds to a shorter H···N distance and a greater elongation of the O–H covalent bond. Figure 1 also shows three cases of transition

TABLE 1: N–H Bonds and H···N Contacts' Distances (Å) and Topological Parameters (au); Electron Density at Corresponding (N–H/H···N) BCP and Laplacian and Energetic Topological Parameters (G_{BCP} , Electron Kinetic Energy Density at BCP; V_{BCP} , Electron Potential Energy Density at BCP; H_{BCP} , Total Electron Energy Density at BCP)^a

derivative	N–H/H···N	$\rho_{\text{NH/H}\cdots\text{N}}$	$\nabla^2\rho_{\text{NH/H}\cdots\text{N}}$	G_{BCP}	V_{BCP}	H_{BCP}
Li,H-A ^b	1.024	0.3271	−1.6875	0.0477	−0.5172	−0.4696
F,H-A ^c	1.031	0.3144	−1.7018	0.0464	−0.5186	−0.4717
H,H-A	1.022	0.326	−1.7567	0.0455	−0.5301	−0.4847
BeH,H-A ^d	1.02	0.3312	−1.7111	0.0456	−0.5189	−0.4733
H,F-A	1.024	0.32	−1.8462	0.0409	−0.5434	−0.5025
H,Li-A	1.028	0.3264	−1.5507	0.0549	−0.4974	−0.4425
H,BeH-A	1.033	0.3179	−1.5675	0.0511	−0.4941	−0.4430
F,F-A ^c	1.037	0.3087	−1.7111	0.0444	−0.5166	−0.4722
F,Li-A ^{c,e}	1.026	0.3221	−1.6157	0.0514	−0.5068	−0.4553
F,BeH-A ^c	1.044	0.3044	−1.4947	0.0518	−0.4772	−0.4254
Li,F-A ^b	1.023	0.3256	−1.8401	0.0412	−0.5425	−0.5013
Li,Li-A ^b	1.025	0.3284	−1.6027	0.0527	−0.5060	−0.4534
Li,BeH-A ^b	1.019	0.329	−1.6646	0.0476	−0.5114	−0.4638
BeH,F-A ^d	1.021	0.3275	−1.8548	0.0393	−0.5422	−0.5030
BeH,Li-A ^{d,f}	1.022	0.3327	−1.5594	0.0524	−0.4947	−0.4423
BeH,BeH-A ^d	1.025	0.3274	−1.5827	0.0498	−0.4953	−0.4455
F,H-B ^c	1.625	0.0646	0.1109	0.0465	−0.0652	−0.0187
H,H-B	1.615	0.0666	0.1061	0.0469	−0.0672	−0.0203
H,F-B	1.767	0.0436	0.1119	0.0335	−0.0389	−0.0055
F,H-TS ^c	1.25	0.1689	−0.2782	0.0708	−0.2112	−0.1404
H,H-TS	1.31	0.1451	−0.1266	0.0700	−0.1716	−0.1016
H,F-TS	1.159	0.2147	−0.7147	0.0636	−0.3059	−0.2423

^a Different derivatives are taken into account, as first one R₁ substituent is indicated; next there is R₂ and the type of tautomer (A, B or TS state).

^b There is additional intramolecular Li···O interaction. ^c There is additional intramolecular F···O interaction. ^d There is additional intramolecular Be···O interaction. ^e There is additional intramolecular Li···F interaction. ^f There is additional intramolecular Li···H interaction (hydride bonding).

TABLE 2: O–H Bonds and H···O Contacts, Distances (Å), and Topological Parameters (au); Electron Density at Corresponding (O–H/H···O) BCP and Its Laplacian and Energetic Topological Parameters (G_{BCP} , Electron Kinetic Energy Density at BCP; V_{BCP} , Electron Potential Energy Density at BCP; H_{BCP} , Total Electron Energy Density at BCP)^a

derivative	O–H/H···O	$\rho_{\text{OH/H}\cdots\text{O}}$	$\nabla^2\rho_{\text{OH/H}\cdots\text{O}}$	G_{BCP}	V_{BCP}	H_{BCP}
Li,H-A ^b	1.879	0.0328	0.1174	0.028	−0.0268	0.0013
F,H-A ^c	1.759	0.0433	0.139	0.0368	−0.0388	−0.002
H,H-A	1.884	0.0325	0.1156	0.0276	−0.0262	0.0013
BeH,H-A ^d	2.107	0.0201	0.071	0.0157	−0.0137	0.002
H,F-A	1.854	0.0358	0.1248	0.0303	−0.0293	0.0009
H,Li-A	1.906	0.0315	0.1078	0.026	−0.025	0.001
H,BeH-A	1.832	0.0366	0.1214	0.0305	−0.0306	−0.0001
F,F-A ^c	1.712	0.049	0.1426	0.0404	−0.0452	−0.0048
F,Li-A ^{c,e}	1.911	0.0315	0.1075	0.0258	−0.0247	0.0011
F,BeH-A ^c	1.71	0.0489	0.1419	0.0404	−0.0454	−0.0049
Li,F-A ^b	1.95	0.0292	0.1075	0.0246	−0.0223	0.0023
Li,Li-A ^b	1.883	0.0329	0.1154	0.0279	−0.0269	0.001
Li,BeH-A ^b	2.142	0.0196	0.07	0.0155	−0.0136	0.002
BeH,F-A ^d	2.086	0.0224	0.0797	0.0177	−0.0155	0.0022
BeH,Li-A ^{d,f}	2.348	0.0128	0.0411	0.0093	−0.0084	0.001
BeH,BeH-A ^d	2.103	0.0203	0.0698	0.0157	−0.0139	0.0018
F,H-B ^c	1.014	0.3072	−2.0493	0.0701	−0.6525	−0.5824
H,H-B	1.022	0.3	−1.9666	0.0704	−0.6324	−0.562
H,F-B	0.99	0.3323	−2.3337	0.0645	−0.7124	−0.6479
F,H-TS ^c	1.224	0.1679	−0.2185	0.0923	−0.2391	−0.1469
H,H-TS	1.173	0.1929	−0.4779	0.0917	−0.3028	−0.2112
H,F-TS	1.352	0.1198	0.067	0.08	−0.1433	−0.0633

^a Different derivatives are taken into account, as first one R₁ substituent is indicated and next there is R₂ and the type of tautomer (a or b) or TS state. ^b There is additional intramolecular Li···O interaction. ^c There is additional intramolecular F···O interaction. ^d There is additional intramolecular Be···O interaction. ^e There is additional intramolecular Li···F interaction. ^f There is additional intramolecular Li···H interaction (hydride bonding).

states considered in this study, for which H···N and H···O distances amount approximately to 1.1–1.3 Å.

The strength of any pair of interacting atoms is reflected by the electron density at the corresponding bond critical point; this density is greater for shorter distances.^{12c} It is shown in Figure 2, where the distance–electron density exponential relationships for H···O/O–H and H···N/N–H interactions were found. The correlations' coefficients for both dependencies are very close to unity (squares of coefficients are given in Figure 2). Hence the distance–electron density dependence implies the

correlation presented in Figure 3: the electron density at H···N/N–H BCP vs the electron density at O–H/H···O BCP for the same H-bond–N–H···O or O–H···N. In the first case of hydrogen bonding there is the relation between electron density at N–H BCP and the electron density at H···O BCP. In the second case of O–H···N this concerns O–H bond and H···N contact.

Figure 4 presents the relationship between the H···O(N) distance and the Laplacian of electron density at the corresponding bond critical point. It indicates the region of covalent

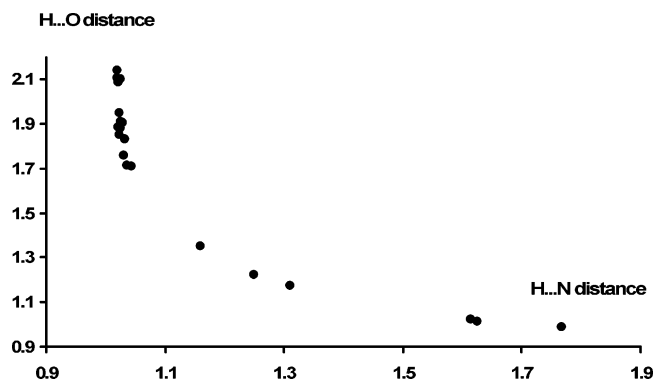


Figure 1. Relationship between N–H/H \cdots N and H \cdots O/O–H distances (both in angstroms).

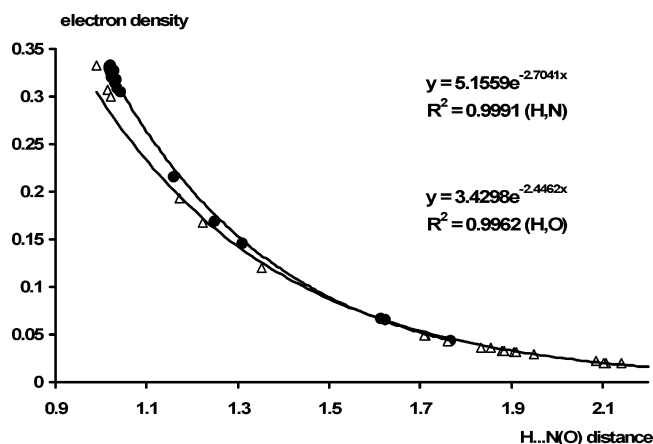


Figure 2. Distance (Å) vs the electron density (au) at the corresponding BCP dependence. The exponential regressions and squares of the correlation coefficients are included.

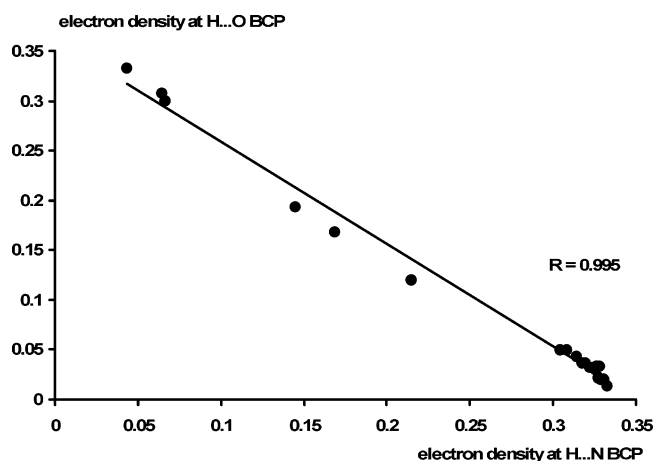


Figure 3. Linear correlation between the electron density at N–H/H \cdots N BCP and the electron density at the corresponding H \cdots O/O–H BCP (both values in au).

bonds where the Laplacian is negative. Figure 4 presents TSs also possessing negative Laplacians. There is only one case of the positive Laplacian value at H \cdots O BCP for the transition state with $R_1 = \text{H}$ and $R_2 = \text{F}$; it is equal to 0.067 au. The H_{BCP} value for this BCP is negative and amounts to -0.0633 au. However for the latter case of hydrogen bonding the corresponding H \cdots N BCP within the same N \cdots H \cdots O system indicates the negative value of Laplacian of -0.7147 au. One can be referred to the last lines of Tables 1 and 2 to compare the values mentioned above.

Summarizing, for N \cdots H \cdots O systems of TSs all contacts indicate negative Laplacians corresponding to the covalent char-

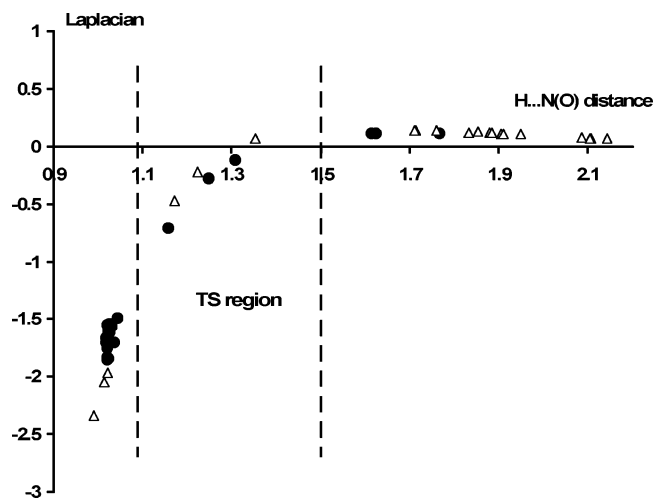


Figure 4. Relationship between H \cdots O(N) distance and the Laplacian of the electron density at the corresponding BCP: full circles, NH/H \cdots N interactions; open triangles, OH/H \cdots O ones. Laplacian, au; distance, Å.

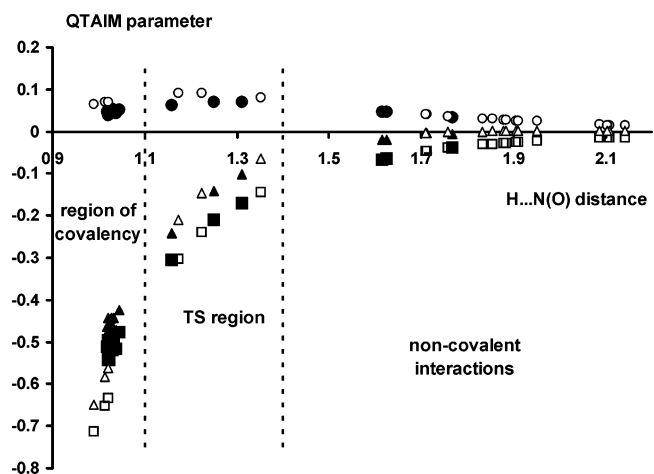


Figure 5. Relationship between the H \cdots O(N) distance and the QTAIM parameter (G_{BCP} , circles; H_{BCP} , triangles; V_{BCP} , squares: open symbols, OH/H \cdots O interactions; filled symbols, NH/H \cdots N ones). QTAIM value, au; distance, Å.

acter of interactions and only in one case of H \cdots O BCP $\nabla^2\rho_{\text{BCP}} > 0$ and $H_{\text{BCP}} < 0$, which means the interaction is at least partly covalent.

Figure 5 shows the relationships between the H \cdots N(O) distance and the other topological parameters such as H_{BCP} , G_{BCP} , and V_{BCP} ; all these topological parameters concern the BCP related to the corresponding bond or contact. One can observe the monotonic AIM parameters' changes with the change of the H \cdots N(O)/O(N)–H distance. V_{C} is always negative, and its modulus increases for shorter distances; G_{C} is always positive and increases if the distance decreases. H_{BCP} is negative for all covalent bonds, all contacts of TSs', and it is positive for H \cdots O within N–H \cdots O systems but negative for H \cdots N contacts for the three B tautomers considered here. The latter is connected with the fact that O–H \cdots N H-bonds are stronger than the corresponding N–H \cdots O H-bonds of the related A tautomeric forms. It results from the Hammond–Leffler¹⁹ postulate that tautomers of the higher total energy possess the stronger H-bonds since they are closer to TSs. It is worth mentioning that H-bonds of TSs are the strongest ones. Generally, for the tautomeric forms of the lower energies the corresponding H-bonds are weaker than H-bonds for tautomers and TSs, which are characterized by higher energies. That was observed for the wide spectrum of systems for which the proton-

TABLE 3: Geometrical Parameters (See Scheme 4), Bond Lengths (Å), and N–H–O Angles (deg)

derivative ^a	d1	d2	d3	d4	N–H–O
Li,H-A ^b	1.244	1.456	1.44	1.324	132.3
F,H-A ^c	1.245	1.467	1.394	1.32	134
H,H-A	1.242	1.461	1.387	1.326	130
Be,H,H-A ^d	1.236	1.448	1.419	1.316	127.4
H,F-A	1.245	1.456	1.387	1.316	123.2
H,Li-A	1.247	1.451	1.413	1.317	139.5
H,BeH-A	1.242	1.464	1.385	1.343	138.9
F,F-A ^c	1.244	1.469	1.387	1.343	133.8
F,Li-A ^{c,e}	1.243	1.464	1.405	1.283	133.6
F,BeH-A ^c	1.245	1.469	1.392	1.325	142
Li,F-A ^b	1.244	1.449	1.435	1.274	119.6
Li,Li-A ^b	1.243	1.459	1.471	1.311	138.3
Li,BeH-A ^b	1.237	1.457	1.416	1.326	121.7
Be,H,F-A ^d	1.238	1.443	1.423	1.286	120.4
Be,H,Li-A ^{d,f}	1.233	1.449	1.452	1.305	127.5
Be,H,BeH-A ^d	1.235	1.451	1.417	1.336	132.8
F,H-B ^c	1.314	1.405	1.452	1.274	147.5
H,H-B	1.315	1.399	1.446	1.29	148.3
H,F-B	1.324	1.393	1.448	1.282	141.5
F,H-TS ^c	1.282	1.431	1.424	1.292	151.5
H,H-TS	1.29	1.418	1.426	1.301	151.8
H,F-TS	1.275	1.431	1.413	1.3	142.8

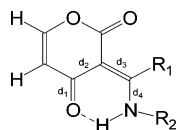
^a The designations of additional contacts (footnotes *b–f* are the same as those in Tables 1 and 2).

transfer process in hydrogen bonds was investigated.⁷ The same is observed for the systems analyzed here.

It was mentioned in early studies that the intramolecular H-bonded systems within the six-membered pseudo-ring possess some unique features.⁶ That is, for example, the equalization of bonds within the six-member pseudo-ring. For O–H···O hydrogen bonds (Scheme 1) the π -electron delocalization leads to the equalization of d1 and d4 (C–O and C=O) bonds on one hand and such equalization of d2 and d3 (C=C and C–C) bonds on the other hand. In other words, the greater the π -electron delocalization is, thus the greater are such equalizations and the greater is the enhancement of the H-bond strength. The latter is also connected with the equalization of the O–H bond length and the H···O distance within the O–H···O system. Besides it was pointed out that R-substituents may also influence the H-bond strength. The enhancement of the latter interaction is connected with the electron-withdrawing features of the R₁-substituent or the electron-donating R₃-substituent (Scheme 1).^{6b}

The influence of the substituents on the hydrogen bonds is analyzed here. Table 3 presents the bond lengths within the pseudo-ring created due to the formation of intramolecular hydrogen bonding. If one compares our systems (Scheme 4) with those considered early by Gilli et al.⁶ (Scheme 1), thus the R₁-substituent should cause similar effects. Fluorine is classified as the electron-withdrawing substituent which increases the H-bond strength if substituted as R₁. And really the H···O distance for such substituted tautomer amounts to 1.759 Å, while this distance for reference A tautomeric form (R₁ = R₂ = H) is equal to 1.884 Å. The proton-acceptor (H···Y) distance as well as the electron density at the H···Y BCP – $\rho_{H\cdots Y}$ is the rough indicator of H-bond strength. The numerous correlations between H-bond energy and the latter topological parameter were found.²¹ For F-substituted A tautomer $\rho_{H\cdots Y} =$

SCHEME 4



0.0443 au, and for the unsubstituted one this is equal to 0.0325 au. For the previous tautomer the equalization of d2 and d3 bonds should be observed as connected with the lengthening of d3 and shortening of d2. Table 3 indicates such equalization but both d₂ and d₃ bonds are elongated for F-substituted species. This may be connected with the other features of F-substituent which is also the π -electron lone pair donating one.²² The latter property probably disturbs the expected results for A tautomer with R₁ = H and R₂ = F. The F-atom at the R₂ position, as an electron-withdrawing substituent, should cause the decrease of the proton affinity of nitrogen and hence the enhancement of the H-bond strength. Such behavior is in line with the rule of the minimum proton affinity difference between the proton donor and the proton acceptor in hydrogen bonds. This is also equivalent to the statement of the minimum difference between the pK_a values of the two interacting groups as measured in a proper polar solvent.^{2,23} However for the mentioned above F-substituted A tautomer its geometrical and topological parameters do not differ significantly if compared with the unsubstituted species (see Tables 1–3). The similar situation is observed if R₁ = Li—no meaningful change of H-bond strength if it is compared with the reference A tautomer (R₁ = R₂ = H), the $\rho_{H\cdots O}$ values are equal to 0.0328 and 0.0325 au, respectively. The influence of the other substituents is also not in line with the simple rules proposed early on,^{6b} but it may be justified since the sample considered here contains more complicated species. The considered intramolecular H-bonds are heteronuclear ones, and also the various other effects should be taken into account.

Analysis of Ring Critical Point Properties. The numerous dependences are known from literature between the geometrical and topological parameters. They mainly concern relationships between the bond length (and the contact distance) and the characteristics of the corresponding bond critical point. However the characteristics of the other critical points are also analyzed from time to time. For example it was found that the ring critical point (RCP) properties may be often treated as measures of the hydrogen bond strength.^{8a,24} Even, very recently, the cage critical point (CCP) properties were investigated and the dependence of the electron density at CCP on the interplane benzene dimer distance was found.²⁵

For the systems analyzed here the pseudo-ring containing N–H···O or O–H···N intramolecular hydrogen bond is created and hence also the RCP exists. The characteristics of RCPs of the systems analyzed here are given in Table 4. It is known that the greater electron density at RCP corresponds to the stronger intramolecular hydrogen bonding since the correlations between the latter value and the $\rho_{H\cdots Y}$ values or the proton-acceptor distance were detected.²⁴ It is worth mentioning that similar relationships are also known for the intermolecular H-bonds of carboxylic acids.²⁶ This may be observed since carboxylic acids form centrosymmetric dimers with two equivalent O–H···O bonds, and hence the eight-member ring is created²⁷ with RCP inside. In other words the properties of the latter critical point are related to the other energetic and geometrical properties of the formed hydrogen bonds. Briefly summarizing, the greater electron density at RCP of intramolecular H-bond corresponds to the stronger interaction.

Figure 6 presents the relationship between the electron density at X–H/H···Y (X–H = N–H, O–H; H···Y = H···O, H···N) BCP and the electron density at the corresponding RCP. One can observe three regions of interactions. For the lowest values of the electron density at BCP there is the increase of ρ_{RCP} if the previous value increases. This is connected with the

TABLE 4: Characteristics of RCPs (au)

derivative ^a	ρ_{RCP}	$\nabla^2\rho_{\text{RCP}}$	V_{RCP}	G_{RCP}	H_{RCP}
Li,H-A ^b	0.0156	0.0976	-0.0153	0.0199	0.0045
F,H-A ^c	0.0170	0.1115	-0.0174	0.0226	0.0053
H,H-A	0.0156	0.0980	-0.0152	0.0199	0.0035
BeH,H-A ^d	0.0126	0.0729	-0.0114	0.0148	0.0034
H,F-A	0.0167	0.1040	-0.0162	0.0211	0.0049
H,Li-A	0.0158	0.0943	-0.0152	0.0194	0.0042
H,BeH-A	0.0164	0.1019	-0.0162	0.0208	0.0046
F,F-A ^c	0.0177	0.1152	-0.0180	0.0234	0.0054
F,Li-A ^{c,e}	0.0166	0.0975	-0.0157	0.0200	0.0043
F,BeH-A ^c	0.0183	0.1169	-0.0187	0.0240	0.0053
Li,F-A ^b	0.0165	0.0963	-0.0151	0.0196	0.0045
Li,Li-A ^b	0.0159	0.0963	-0.0154	0.0198	0.0043
Li,BeH-A ^b	0.0134	0.0734	-0.0117	0.0150	0.0034
BeH,F-A ^c	0.0140	0.0794	-0.0123	0.0161	0.0038
BeH,Li-A ^{d,f}	0.0100	0.0506	-0.0083	0.0105	0.0022
BeH,BeH-A ^d	0.0127	0.0720	-0.0115	0.0147	0.0033
F,H-B ^c	0.0199	0.1288	-0.0206	0.0264	0.0058
H,H-B	0.0199	0.1312	-0.0212	0.0270	0.0058
H,F-B	0.0170	0.1062	-0.0165	0.0215	0.0051
F,H-TS ^c	0.0235	0.1622	-0.0269	0.0337	0.0068
H,H-TS	0.0234	0.1621	-0.0270	0.0337	0.0068
H,F-TS	0.0223	0.1532	-0.0248	0.0315	0.0068

^a The designations of additional contacts (footnotes *b–f* are the same as those in Tables 1 and 2).

shortening of nonbonding contact, H \cdots O or H \cdots N. Thus the greater the electron density is at BCP for the shorter contact and the stronger H-bond interaction so the greater is the ρ_{RCP} value. The second region concerns the contacts of transition states. Both electron densities at RCP and BCP in such a case are generally greater than for the previous nonbonding region. This is connected with the well-known observation that H-bonds for transition states are very strong.⁷ For the latter region both H \cdots O and H \cdots N interactions are taken into account. And the last region concerns N–H and O–H covalent bonds. The elongation of covalent bonds causes the decrease of the electron density at the corresponding BCP (Figure 6, X-axis) and the increase of ρ_{RCP} . It means that hydrogen bonds become stronger interactions. One can see that there are correlations between the ρ_{RCP} and the $\rho_{\text{OH/NH}}$ on one hand and also between ρ_{RCP} and $\rho_{\text{H}\cdots\text{N/H}\cdots\text{O}}$ on the other hand. For both subsamples of atom–atom distances good correlations are observed (Figure 6).

It is worth mentioning that all topological parameters may be used as descriptors of the H-bond strength since there is an increase of all characteristics of RCP for stronger interactions. All correlate between themselves, and the linear correlation coefficients are close to the unity (Table 5).

Transition State and the Proton-Transfer Process. It was mentioned in the previous section that the proton-transfer process N–H \cdots O \rightleftharpoons N \cdots H–O concerns two corresponding (A and B)

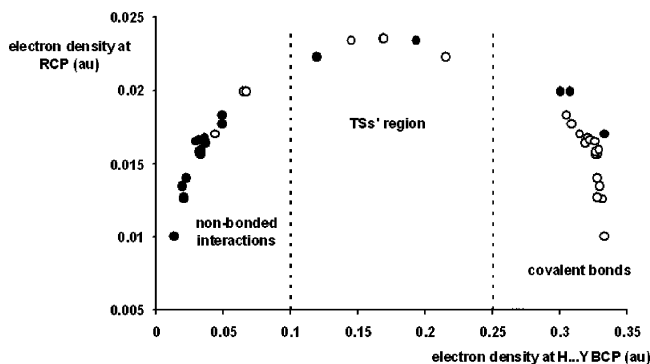


Figure 6. Relationship between ρ_{BCP} and ρ_{RCP} (both in au). Filled circles correspond to OH/H \cdots O interactions; open circles, to NH/H \cdots N.

TABLE 5: Linear Correlation Coefficients of the Different Relationships between the Characteristics of the Ring Critical Point

	ρ_{RCP}	$\nabla^2\rho_{\text{RCP}}$	V_{RCP}	G_{RCP}	H_{RCP}
ρ_{RCP}	1	0.995	0.993	0.995	0.974
$-\nabla^2\rho_{\text{RCP}}$		1	0.997	1	0.976
V_{RCP}			1	0.999	0.967
G_{RCP}				1	0.972
H_{RCP}					1

TABLE 6: Energies (hartrees) of the Species Analyzed Here^a

derivative	energy	energy difference
F,H-A	−611.489 039	3.94 ^b
F,H-B	−611.486 590	2.41 ^b
F,H-TS	−611.482 753	1.54 ^c
H,H-A	−512.224 399	7.77 ^b
H,H-B	−512.213 963	1.22 ^b
H,H-TS	−512.212 014	6.55 ^c
H,F-A	−611.405 360	2.06 ^b
H,F-B	−611.416 151	8.84 ^b
H,F-TS	−611.402 070	−6.77 ^c

^a The energies of A and B tautomeric forms as well as of transition states are given. The energy differences are also presented (kcal/mol).
^b $E_{\text{TS}} - E(\text{A or B})$. ^c $E(\text{B}) - E(\text{A})$.

tautomeric forms (Scheme 3) and that for three species the DFT calculations were performed here for both A and B tautomers as well as for the corresponding transition states. Their geometrical and topological results are given in Tables 1–3. Since for three A tautomeric forms the corresponding B tautomers are considered and also the TSs of the proton-transfer reaction, thus there are nine related molecular species, and their energies are given in Table 6. The energies of A and B correspond to minima (no imaginary frequencies observed). One can observe that in two cases the A tautomeric form is of the lower energy than the B counterpart. The energy differences are also presented in Table 6. Such a difference between B and A tautomeric forms for unsubstituted species amounts to 6.6 kcal/mol. There is one case where B tautomer is of lower energy than the A counterpart; this is for $R_2 = \text{F}$. In other words the species with the O–H \cdots N hydrogen bond is of lower energy than that one where the N–H \cdots O hydrogen bond exists since the latter tautomer is closer to the corresponding transition state.

The situation for all three cases considered here may be explained in the following way. Nitrogen is of greater proton affinity than oxygen atom; hence, N–H \cdots O systems exist in the species of lower energy. The systems with O–H \cdots N are of the higher energies than the previous ones. On the other hand the latter have the stronger H-bonds and are close to TSs. For the transition states H-bonds are the strongest. For $R_2 = \text{F}$ the proton affinity of nitrogen decreases since F is the electron-withdrawing substituent. In consequence the proton affinity for oxygen is greater than for nitrogen. As a result of such a situation the B tautomer is of lower energy than the A form by 6.8 kcal/mol. It is worth mentioning that the potential barrier heights for all species are in the range of 1.5–6.8 kcal/mol

Other Intramolecular Interactions. Since there are few oxygen acceptor centers in the species considered here and also the derivatives with such substituents as –F, –Li, and –BeH are included, thus it implies the existence of various intramolecular interactions. Except of intramolecular hydrogen bonds, these are $\text{Li}^{+\delta}\cdots\text{O}^{-\delta}$, $\text{Be}^{+\delta}\cdots\text{O}^{-\delta}$, $\text{Li}^{+\delta}\cdots\text{F}^{-\delta}$, and $\text{Li}^{+\delta}\cdots\text{H}^{-\delta}$ ionic interactions as well as an O \cdots F one. Table 7 presents the characteristics of the corresponding BCPs. These are electron densities at BCPs and their Laplacians. If one assumes that such values reflect the strength of interaction, thus $\text{Be}^{+\delta}\cdots\text{O}^{-\delta}$'s is

TABLE 7: Other Intramolecular Interactions and ρ_{BCP} and $\nabla^2\rho_{\text{BCP}}$ for These Interactions (au)^a

derivative ^b	type of interaction	ρ_{BCP}	$\nabla^2\rho_{\text{BCP}}$
Li,H-A	Li \cdots O	0.0411	0.3087
F,H-A	F \cdots O	0.0139	0.0581
BeH,H-A	Be \cdots O	0.0728	0.4968
F,F-A	F \cdots O	0.0128	0.0544
F,Li-A	F \cdots O	0.0146	0.0605
F,Li-A	Li \cdots F	0.0257	0.1840
F,BeH-A	F \cdots O	0.0143	0.0599
Li,F-A	Li \cdots O	0.0400	0.2949
Li,Li-A	Li \cdots O	0.0483	0.3743
Li,BeH-A	Li \cdots O	0.0411	0.3065
BeH,F-A	Be \cdots O	0.0744	0.5031
BeH,Li-A	Be \cdots O	0.0910	0.6269
BeH,Li-A	Li \cdots H	0.0191	0.0735
BeH,BeH-A	Be \cdots O	0.0737	0.5046
F,H-B	F \cdots O	0.0137	0.0567
F,H-TS	F \cdots O	0.0121	0.0500

^a The tautomeric form (A or B) and TS are indicated. ^b For italicized derivatives, except for hydrogen bonding, two additional interactions exist.

the strongest one since $\rho_{\text{Be}\cdots\text{O}}$'s values are in the range of 0.0728–0.0910 au. For example, for the trans-linear dimer of water where the H-bond energy is estimated as ~ 5 kcal/mol, the $\rho_{\text{H}\cdots\text{O}}$ calculated at the same level of approximation as the systems considered here (B3LYP/6-311++G(d,p)) is equal to 0.024 au.²⁸ The next strong interaction is Li $^{\delta+}\cdots^{\delta-}\text{O}$, with a $\rho_{\text{Li}\cdots\text{O}}$ of 0.0400–0.0483 au; that is even stronger than Li $^{\delta+}\cdots^{\delta-}\text{F}$ since $\rho_{\text{Li}\cdots\text{F}}$ for a single case amounts to 0.0257 au. There is also the Li $^{\delta+}\cdots^{\delta-}\text{H}$ interaction where the electron density at the corresponding BCP is equal to 0.0191 au, close to the value of the water dimer. It means the Li $^{\delta+}\cdots^{\delta-}\text{H}$ –Be interaction is not negligible. That may be also classified as the intramolecular hydride bonding. Intermolecular hydride bonds (named first as inverse H-bonds) were analyzed in earlier studies²⁹ as well as very recently.³⁰ Such interactions are characterized by the X–H \cdots Y system where X and Y are electropositive atoms while the hydrogen atom is negatively charged, opposite to typical hydrogen bonding. Figure 7a presents the molecular graph of the derivative where R₁ and R₂ substituents are –BeH and –Li, respectively, and where the Li $^{\delta+}\cdots^{\delta-}\text{H}$ –Be interaction exists. The electron density contour map with the gradient paths is also included (Figure 7b). One can observe that except for N–H \cdots O hydrogen bonding and the Li $^{\delta+}\cdots^{\delta-}\text{H}$ interaction also the Be $^{\delta+}\cdots^{\delta-}\text{O}$ interaction occurs.

The weakest F \cdots O interactions are characterized by rather low values of the electron densities at BCPs, of about 0.012–0.015 au. Since for both contacting atoms there is the negative electron charge excess, thus these interactions may be probably classified as stabilizing ones. Such a situation was discussed in recent studies for H \cdots H interactions³¹ as well as for F \cdots F ones.³²

Summary

The intramolecular N–H \cdots O hydrogen bonds were analyzed here for 3-(aminomethylene)pyran-2,4-dione and its simple derivatives. For some species, unsubstituted reference and fluorine ones, the other tautomeric forms with O–H \cdots N hydrogen bond were investigated. Additionally the transition states of the proton-transfer reaction were taken into account. Numerous continuous H \cdots O and H \cdots N interactions were detected since there is the smooth change of all geometrical and topological parameters if different relationships are considered. It means that there is no the sharp border between the H-bond and the covalent bond; strictly speaking, the hydrogen bonds are “interactions without borders”.³³

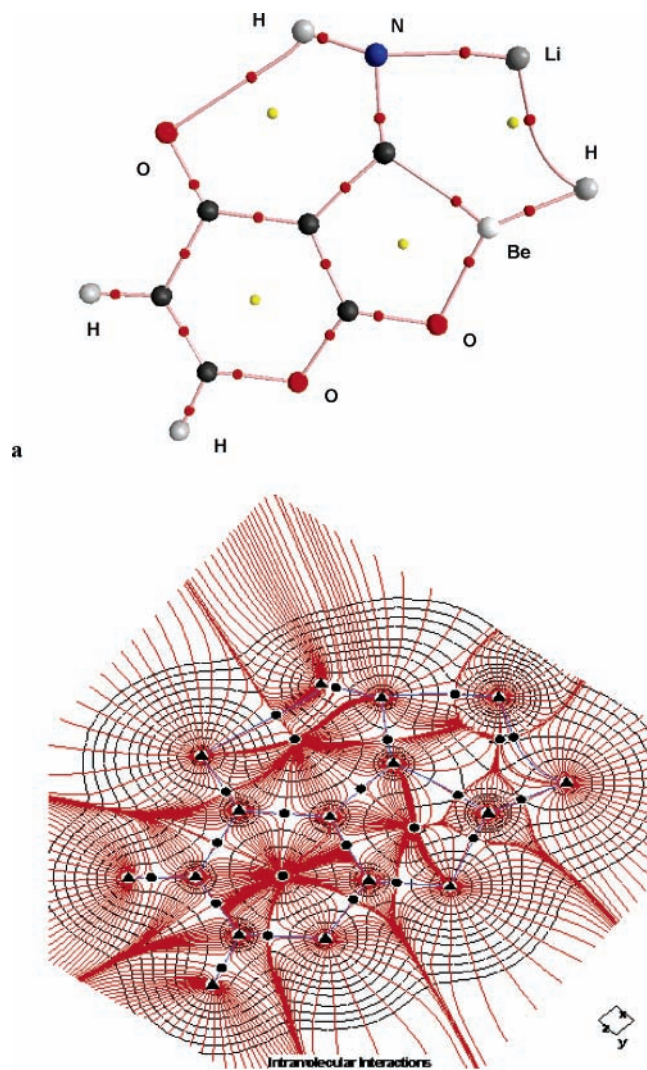


Figure 7. (a) Molecular graph of the derivative with R₁ = BeH and R₂ = Li. Some of the atoms are designated; the remaining are carbon ones. (b) Contour map of the electron density (black lines) of the species with the gradient paths (red lines). Triangles correspond to the attractors; circles, to the bond and ring critical points. The orientation and the positions of the atoms and critical points are the same as in a.

The influence of substituents on H-bond strength was analyzed. It was found for the systems investigated here that F-atom attached to nitrogen participating in the N–H \cdots O H-bond, causing the tautomeric form with the O–H \cdots N hydrogen bond to be more stable than the previous form. This is the result of the decrease of the proton affinity of nitrogen since fluorine is the electron-withdrawing substituent.

It was also found that the characteristics of RCP are good descriptors of the H-bond strength. They correlate well between themselves and with the other H-bond strength measures. Except for intramolecular H-bonds, the other intramolecular interactions were analyzed here; also the unique Be–H \cdots Li interaction was detected.

Acknowledgment. Support has been provided by Grant No. 505/706 2006 (University of Łódź), the State Committee for Scientific Research (KBN No. 3T09A 138 26). Use of computational resources of the Cracow Supercomputing Center is also acknowledged.

References and Notes

- (1) Jeffrey, G. A.; Saenger, W. *Hydrogen Bonding in Biological Structures*; Springer: Berlin, 1991.
- (2) Sobczyk, L.; Grabowski, S. J.; Krygowski, T. M. *Chem. Rev.* **2005**, *105*, 3513.
- (3) Buemi, G. Hydrogen Bonding—New Insights. In *Intramolecular Hydrogen Bonds. Methodologies and Strategies for Their Strength Evaluation*; Grabowski, S. J., Ed.; Springer: Berlin, 2006.
- (4) Etter, M. C. *Acc. Chem. Res.* **1990**, *23*, 120.
- (5) Grabowski, S. J. *J. Phys. Org. Chem.* **2003**, *16*, 797.
- (6) (a) Gilli, G.; Belluci, F.; Ferretti, V.; Bertolesi, V. *J. Am. Chem. Soc.* **1989**, *111*, 1023. (b) Bertolasi, V.; Gilli, P.; Ferretti, V.; Gilli, G. *J. Am. Chem. Soc.* **1991**, *113*, 4917. (c) Gilli, P.; Bertolasi, V.; Ferretti, V.; Gilli, G. *J. Am. Chem. Soc.* **1994**, *116*, 909. (d) Gilli, G.; Gilli, P. *J. Mol. Struct.* **2000**, *552*, 1.
- (7) (a) Gilli, P.; Bertolasi, V.; Ferretti, V.; Gilli, G. *J. Am. Chem. Soc.* **2000**, *122*, 10405. (b) Gilli, P.; Bertolasi, V.; Pretto, L.; Lyčka, A.; Gilli, G. *J. Am. Chem. Soc.* **2002**, *124*, 13554. (c) Gilli, P.; Bertolasi, V.; Pretto, L.; Ferretti, V.; Gilli, G. *J. Am. Chem. Soc.* **2004**, *126*, 3845.
- (8) (a) Rybarczyk-Pirek, A. J.; Grabowski, S. J.; Małecka, M.; Nawrot-Modranka, J. *J. Phys. Chem. A* **2002**, *106*, 11956. (b) Rybarczyk-Pirek, A. J.; Grabowski, S. J.; Nawrot-Modranka, J. *J. Phys. Chem. A* **2003**, *107*, 9232. (c) Małecka, M.; Grabowski, S. J.; Budzisz, E. *Chem. Phys.* **2004**, *297*, 235. (d) Rybarczyk-Pirek, A. J.; Dubis, A. T.; Grabowski, S. J.; Nawrot-Modranka, J. *Chem. Phys.* **2006**, *320*, 247.
- (9) (a) Leiserowitz, L. *Acta Crystallogr.* **1976**, *B32*, 775. (b) Gora, R. W.; Grabowski, S. J.; Leszczynski, J. *J. Phys. Chem. A* **2005**, *109*, 6397. (c) Grabowski, S. J.; Sokalski, W. A.; Leszczynski, J. *J. Phys. Chem. A* **2006**, *110*, 4772. (d) Grabowski, S. J.; Dubis, A. T.; Palusiak, M.; Leszczynski, J. *J. Phys. Chem. B* **2006**, *110*, 5875.
- (10) (a) Alkorta, I.; Elguero, J.; M^o, O.; Yáñez, M.; del Bene, J. E. *Mol. Phys.* **2004**, *102*, 2563. (b) Alkorta, I.; Elguero, J.; M^o, O.; Yáñez, M.; del Bene, J. E. *Chem. Phys. Lett.* **2002**, *411*, 411.
- (11) (a) Filarowski, A.; Koll, A.; Głowiak, T. *J. Chem. Soc. Perkin Trans. 2* **2002**, 835. (b) Filarowski, A.; Koll, A. *Vib. Spectrosc.* **1998**, *17*, 123. (c) Filarowski, A.; Koll, A.; Głowiak, T.; Majewski, E.; Dziembowska, T. *Ber. Bunsen-Ges. Phys. Chem.* **1998**, *102*, 393. (d) Filarowski, A.; Koll, A.; Głowiak, T. *Monatsh. Chem.* **1999**, *130*, 1097. (e) Filarowski, A.; Koll, A.; Karpfen, A.; Wolschann, P. *Chem. Phys.* **2004**, *297*, 323.
- (12) (a) Bader, R. F. W. *Acc. Chem. Res.* **1985**, *18*, 9. (b) Bader, R. F. W. *Chem. Rev.* **1991**, *91*, 893. (c) Bader, R. F. W. *Atoms in Molecules, A Quantum Theory*; Oxford University Press: Oxford, U.K., 1990.
- (13) (a) Parr, R. G.; Yang, W. *Density Functional Theory of Atoms and Molecules*; Oxford: New York, 1989. (b) Dreizler, R. M.; Gross, E. K. V. *Density Functional Theory*; Springer: Berlin, 1990. (c) Kohn, W.; Becke, A. D.; Parr, R. G. *J. Phys. Chem.* **1996**, *100*, 12974. (d) Müller-Dethlefs, K.; Hobza, P. *Chem. Rev.* **2000**, *100*, 143. (e) Chalasinski, G.; Szczyński, M. M. *Chem. Rev.* **2000**, *100*, 4227.
- (14) Frisch, M. J.; Trucks, G. W.; Schlegel, H. B.; Scuseria, G. E.; Robb, M. A.; Cheeseman, J. R.; Montgomery, J. A., Jr.; Vreven, T.; Kudin, K. N.; Burant, J. C.; Millam, J. M.; Iyengar, S. S.; Tomasi, J.; Barone, V.; Mennucci, B.; Cossi, M.; Scalmani, G.; Rega, N.; Petersson, G. A.; Nakatsuji, H.; Hada, M.; Ehara, M.; Toyota, K.; Fukuda, R.; Hasegawa, J.; Ishida, M.; Nakajima, T.; Honda, Y.; Kitao, O.; Nakai, H.; Klene, M.; Li, X.; Knox, J. E.; Hratchian, H. P.; Cross, J. B.; Bakken, V.; Adamo, C.; Jaramillo, J.; Gomperts, R.; Stratmann, R. E.; Yazyev, O.; Austin, A. J.; Cammi, R.; Pomelli, C.; Ochterski, J. W.; Ayala, P. Y.; Morokuma, K.; Voth, G. A.; Salvador, P.; Dannenberg, J. J.; Zakrzewski, V. G.; Dapprich, S.; Daniels, A. D.; Strain, M. C.; Farkas, O.; Malick, D. K.; Rabuck, A. D.; Raghavachari, K.; Foresman, J. B.; Ortiz, J. V.; Cui, Q.; Baboul, A. G.; Clifford, S.; Cioslowski, J.; Stefanov, B. B.; Liu, G.; Liashenko, A.; Piskorz, P.; Komaromi, I.; Martin, R. L.; Fox, D. J.; Keith, T.; Al-Laham, M. A.; Peng, C. Y.; Nanayakkara, A.; Challacombe, M.; Gill, P. M. W.; Johnson, B.; Chen, W.; Wong, M. W.; Gonzalez, C.; Pople, J. A. *Gaussian 03*, Revision B.03; Gaussian, Inc.: Wallingford, CT, 2004.
- (15) Krishnam, R.; Binkley, J. S.; Seeger, R.; Pople, J. A. *J. Chem. Phys.* **1984**, *80*, 3265.
- (16) Becke, A. D. *J. Chem. Phys.* **1993**, *98*, 5648.
- (17) Cremer, D.; Kraka, E. *Angew. Chem., Int. Ed. Engl.* **1984**, *23*, 627.
- (18) Rozas I, Alkorta I, Elguero J. *J. Am. Chem. Soc.* **2000**, *122*, 11154.
- (19) (a) Leffler, J. E. *Science* **1953**, *117*, 340. (b) Hammond, G. S. *J. Am. Chem. Soc.* **1955**, *77*, 334.
- (20) (a) Jeffrey, G. A. *An Introduction to Hydrogen Bonding*; Oxford University Press: New York, 1997. (b) Desiraju, G. R.; Steiner, T. *The Weak Hydrogen Bond in Structural Chemistry and Biology*; Oxford University Press: New York, 1999.
- (21) (a) M^o, O.; Yáñez, M.; Elguero, J. *J. Chem. Phys.* **1992**, *97*, 6628. (b) M^o, O.; Yáñez, M.; Elguero, J. *J. Mol. Struct. (THEOCHEM)* **1994**, *314*, 73. (c) Espinosa, E.; Molins, E.; Lecomte, C. *Chem. Phys. Lett.* **1998**, *285*, 170. (d) Galvez, O.; Gomez, P. C.; Pacios, L. F. *Chem. Phys. Lett.* **2001**, *337*, 263. (e) Galvez, O.; Gomez, P. C.; Pacios, L. F. *J. Chem. Phys.* **2001**, *115*, 11166. (f) Galvez, O.; Gomez, P. C.; Pacios, L. F. *J. Chem. Phys.* **2003**, *118*, 4878. (g) Pacios, L. F. *J. Phys. Chem. A* **2004**, *108*, 1177. (h) Pacios, L. F. *Struct. Chem.* **2005**, *16*, 223.
- (22) Lo, S.-J.; Li, W.-S.; Chan, Y.-H.; Chao, I. *Chem. Eur. J.* **2005**, *11*, 6533.
- (23) (a) Malarski, Z.; Rospenk, M.; Sobczyk, L.; Grech, E. *J. Phys. Chem.* **1982**, *86*, 401. (b) Zeegers-Huyskens, T. In *Intermolecular Forces*; Huyskens, P. L., Luck, W. A., Zeegers-Huyskens, T., Eds.; Springer: Berlin, 1991; Chapter 6. (c) Sobczyk, L. *Ber. Bunsen-Ges. Phys. Chem.* **1998**, *102*, 377. (d) Reinhard, L. A.; Sacksteder, K. A.; Cleland, W. A. *J. Am. Chem. Soc.* **1998**, *120*, 13366.
- (24) Grabowski, S. J. *Monatsh. Chem.* **2002**, *133*, 1373.
- (25) Zhikol, O. A.; Shishkin, O. V.; Lyssenko, K. A.; Leszczynski, J. *J. Chem. Phys.* **2005**, *122*, 144104.
- (26) Dubis, A. T.; Grabowski, S. J.; Romanowska, D. B.; Misiaszek, T.; Leszczynski, J. *J. Phys. Chem. A* **2002**, *106*, 10613.
- (27) Staab, H. A. *Einführung in die Theoretische Organische Chemie*; Verlag Chemie: Weinheim/Bergstrasse, Germany, 1959.
- (28) Domagała, M.; Grabowski, S. J.; Urbaniak, K.; Młostoń, G. *J. Phys. Chem. A* **2003**, *107*, 2730.
- (29) (a) Rozas, I.; Alkorta, I.; Elguero, J. *J. Phys. Chem. A* **1997**, *101*, 4236. (b) Cotton, F. A.; Matonic, J. H.; Murillo, C. A. *J. Am. Chem. Soc.* **1998**, *120*, 6047.
- (30) Grabowski, S. J.; Sokalski, W. A.; Leszczynski, J. *Chem. Phys. Lett.* **2006**, *422*, 334.
- (31) (a) Matta, C. F.; Hernández-Trujillo, J.; Tang, T.-H.; Bader, R. F. W. *Chem.—Eur. J.* **2003**, *9*, 1940. (b) Matta, C. F. *Hydrogen Bonding—New Insights. In Hydrogen—Hydrogen Bonding; the Non-electrostatic Limit of Closed-Shell Interaction Between Two Hydrogen Atoms*; Grabowski, S. J., Ed.; Springer: Berlin, 2006.
- (32) Matta, C. F.; Castillo, N.; Boyd, R. J. *J. Phys. Chem. A* **2005**, *109*, 3669.
- (33) Desiraju, G. R. *Acc. Chem. Res.* **2002**, *35*, 565.